Journal of Neuroscience Research 68:46–58 (2002)

Establishment and Characterization of Immortalized Neuronal Cell Lines Derived From the Spinal Cord of Normal and Trisomy 16 Fetal Mice, an Animal Model of Down Syndrome

Ana María Cárdenas,[1] David D. Allen,[2] Christian Arriagada,[3] Alexis Olivares,[1] Lori B. Bennett,[4] Raúl Caviedes,[4] Alexies Dagnino-Subiabre,[4] Isabel E. Mendoza,[1] Juan Segura-Aguilar,[4] Stanley I. Rapoport,[5] and Pablo Caviedes[4,6]*

[1]Laboratory of Pharmacology, School of Medicine and Valparaíso Center for Cellular and Molecular Neuroscience, University of Valparaíso, Valparaíso, Chile
[2]Department of Pharmaceutical Sciences, Texas Tech University HSC, Amarillo, Texas
[3]Program of Morphology, ICBM, Faculty of Medicine, University of Chile, Santiago, Chile
[4]Program of Molecular and Clinical Pharmacology, ICBM, Faculty of Medicine, University of Chile, Santiago, Chile
[5]Section of Brain Physiology and Metabolism, NIA, NIH, Bethesda, Maryland
[6]Sansum Medical Research Institute, Santa Barbara, California

We report the establishment of continuously growing cell lines from spinal cords of normal and trisomy 16 fetal mice. We show that both cell lines, named M4b (derived from a normal animal) and MTh (trisomic) possess neurological markers by immunohistochemistry (neuron specific enolase, synaptophysin, microtubule associated protein-2 [MAP-2], and choline acetyltransferase) and lack glial traits (glial fibrillary acidic protein and S100). MTh cells were shown to overexpress mRNA of Cu/Zn superoxide dismutase, whose gene is present in autosome 16. We also studied intracellular Ca^{2+} signals ($[Ca^{2+}]_i$) induced by different agonists in Indo-1 loaded cells. Basal $[Ca^{2+}]_i$ was significantly higher in MTh cells compared to M4b cells. Glutamate (200 μM) and (1S,3R)-1-aminocyclopentane-1,3-dicarboxylic acid (ACDP) (100 μM) induced rapid, transient increases in $[Ca^{2+}]_i$ in M4b and MTh cells, indicating the presence of glutamatergic metabotropic receptors. N-methyl-D-aspartate (NMDA) and kainate, but not alpha-amino-hydroxy-5-methylisoxazole-4-propionic acid (AMPA), produced $[Ca^{2+}]_i$ rises in both cell types. MTh cells exhibited faster time-dependent decay phase kinetics in glutamate-induced responses compared to M4b cells. Nicotine induced a transient increase in $[Ca^{2+}]_i$ in M4b and MTh cells, with significantly greater amplitudes in the latter compared to the former. Further, both cell types responded to noradrenaline. Finally, we examined cholinergic function in both cell lines and found no significant differences in the [^{3}H]-choline uptake, but fractional acetylcholine release induced by either K^+, glutamate or nicotine was significantly higher in MTh cells. These results show that M4b and MTh cells have neuronal characteristics and the MTh line shows differences which could be related to neuronal pathophysiology in Down's syndrome.

Key words: calcium; glutamate; nicotine; spinal cord; trisomy 21; Down syndrome

Down syndrome is expressed with mental retardation, increased incidence of congenital malformations, a relationship with Alzheimer's disease, and muscle hypotonia. The latter could result from spinal cord dysfunction. Indeed, altered action potential (Orozco et al., 1987) and cholinergic dysfunction (Fiedler et al., 1994) have been observed in cultured spinal cord neurons from trisomy 16 mice, a model of human trisomy 21 (Epstein, 1986; Coyle et al., 1988).

Murine trisomy 16 and human trisomy 21 exhibit altered cell membrane function (Sweeney et al., 1989; Ault et al., 1989a; Caviedes et al., 1990; Fiedler et al.,

Contract grant sponsor: Fondecyt, Chile; Contract grant numbers: 1980906, 7980058, 1990622; Contract grant sponsor: DIPUV (Valparaíso, Chile); Contract grant number: 0398; Contract grant sponsor: Texas Tech University HSC School of Pharmacy.

*Correspondence to: Pablo Caviedes, M.D., Ph.D., Program of Molecular and Clinical Pharmacology, ICBM, Faculty of Medicine, University of Chile, Casilla 70000, Correo 7, Santiago, Chile.
E-mail: pcaviede@machi.med.uchile.cl

Received 12 June 2001; Revised 7 January 2002; Accepted 9 January 2002

1994; Acevedo et al., 1995), possibly related to increased gene dosage effects (Epstein et al., 1985; Epstein, 1986; Ault et al., 1989b; Mattson and Rydel, 1992). Nevertheless, qualitative differences are evident when comparing different territories of the nervous system in the aneuploid condition. In this regard, diverse electrophysiological alterations have been found in neurons of human and mouse aneuploid subjects compared to controls. Indeed, Ault et al. (1989a) and Orozco et al. (1987) reported shorter action potential duration in dorsal root ganglia of trisomy 16 mice, a situation also encountered by Acevedo et al. (1995) in trisomic septal neurons in culture. But Galdzicki et al. (1993) demonstrated increased spike duration in trisomic hippocampal neurons. Further, studies by our group (Fiedler et al., 1994) demonstrated divergent alterations in cholinergic function between cultured trisomic neurons from brain and spinal cord, which could underlie behavior responses to pain in the Ts65Dn mouse (Martínez-Cué et al., 1999), a model which contains an extra segment of chromosome 16 homologous to the Down syndrome region (Reeves et al., 1995) and survives gestation.

Taken together, the studies described above indicate alterations at the neuronal level that may underlie fundamental mechanisms of Down syndrome pathology, but they clearly denote that the higher gene dosage inherent to the trisomic condition affects, in a differential fashion, the neurons of the different regions of the central nervous system. It is therefore desirable to establish cell lines from different territories of the nervous system, specially considering that trisomy 16 animals die in utero. Such permanent, in vitro models could prove beneficial in understanding the effects of the trisomic condition and address the pathophysiological alterations depicted above at the cellular level in every given territory. In this regard, we have previously established continuously growing cell lines from cerebral cortex of a normal and trisomy 16 fetal mouse using the UCHTl protocol (Cárdenas et al., 1999; Allen et al., 2000). To analyze the situation at the spinal cord level, we have now established spinal cord cell lines from normal and trisomy 16 fetal mice with the same procedure. These cell lines (M4b, derived from a normal mouse and MTh, derived from a trisomic animal) were characterized using genetic (RT-PCR), morphological (immunohistochemistry) and neuronal function studies (intracellular Ca^{2+} responses to neurotransmitters, choline uptake and active release). MTh overexpresses Cu/Zn superoxide dismutase (SOD-1), whose gene is present in human autosome 21 and murine 16 (Coyle et al., 1988; Caviedes et al., 1990), suggesting the preservation of the trisomic phenotype. By immunohistochemistry and immunobloting, both cell types exhibit neuronal markers, but lack glial traits. Both lines respond to neurotransmitters with elevations of $[Ca^{2+}]_i$, indicating the presence of functional receptors. Finally, both cell lines incorporate choline from the extracellular medium, but the trisomic cells release more acetylcholine (ACh) in response to external stimuli compared to the normal line. The MTh cell line is presented as a model to study neural pathophysiology in the spinal cord of Down syndrome.

MATERIALS AND METHODS

Cell Culture

Establishment of cell lines. Trisomy 16 and normal fetuses were obtained by breeding double heterozygous (Rb 2H/RB 32 Lub) males with normal C57BL females as described previously (Orozco et al., 1987; Ault et al., 1989a). Pregnant females were anesthetized with CO_2 and killed by cervical dislocation after 12–16 days of gestation. The fetuses were placed in phosphate-buffered saline (PBS) and trisomic fetuses were identified by their characteristic massive edema. Normal (2N) littermates were used as age-matched controls. Whole spinal cords from trisomic and littermate control fetuses were removed and meninges were withdrawn. Tissues were minced and suspended in 3 ml of PBS containing 0.12% (w/v) of trypsin (Sigma, St. Louis, MO) and incubated for 30 min at 37°C. Afterwards, the trypsin reaction was stopped by adding an equal volume of plating medium, consisting of Dulbecco's modified Eagle's medium (DMEM)/Ham's F-12 nutrient mixture (1:1; Sigma) modified to contain 6 g/l glucose, 10% bovine serum, 10% fetal bovine serum, 100 U/ml penicillin, 100 μg/ml streptomycin (Sigma). The suspension was centrifuged and the pellet resuspended in 2 ml of plating medium. The tissue was dissociated by passages through a fire-polished Pasteur pipette, and the cells plated on a collagen (Calbiochem, San Diego, CA)-coated 60-mm culture dish at a density of 40,000 cells/cm^2. At the time of seeding, the plating medium was supplemented with 5% (v/v) of medium conditioned by the UCHT1 rat thyroid cell line (Caviedes and Stanbury, 1976), which reportedly induces transformation in vitro (Caviedes et al., 1993, 1994; Liberona et al., 1997; Cárdenas et al., 1999; Allen et al., 2000).

After 24 hr, the initial plating medium was replaced by feeding medium consisting of DMEM/Ham's F12 nutrient mixture (1:1) modified to contain 6 g/l glucose, 10% bovine serum, 2.5% fetal bovine serum, 100 U/ml penicillin, 100 μg/ml streptomycin (Sigma) and 10% UCHT1 conditioned medium. The cultures were kept in an incubator at 37°C with 100% humidity and an atmosphere of 5% CO_2 and were monitored routinely for appearance of transformation foci or morphological changes, which became evident after variable periods of time (7–8 months) and signaled the establishment of cell lines M4b (derived from normal spinal cord) and MTh (derived from trisomic spinal cord).

Culture of cell lines. For standard growth conditions, M4b and MTh cells were cultured in feeding medium. For recording of Ca^{2+} signals, 25-mm-diameter glass coverslips were previously coated with Matrigel, and incubated at 37°C for 30 min to allow gelification. Later, the cells were plated onto treated surface, at a density of 2.5×10^4 cells/ml.

Reverse Transcription-Polymerase Chain Reaction (RT-PCR) Analysis

The expression of Cu/Zn superoxide dismutase (SOD-1) in the M4b and MTh cell line was studied by using the RT-

PCR technique. Total RNA was isolated, as described previously (Arriagada et al., 2000), by using RNeasy Midi kit (Qiagen, Chatsworth, CA). cDNA was synthesized from 1 μg of total RNA using ThermoScript reverse transcriptase. The PCR was performed in 50 μl of reaction sample containing cDNA (corresponding to 75 ng of total RNA), 2.5 μM of each oligonucleotide primer, 0.4 mM of dNTP, 3 mM $MgCl_2$ and 2 U of Taq polymerase (Gibco BRL, Gaithersburg, MD). The PCR reaction was performed in three steps: (1) 95°C for 5 min; (2) 30 cycles at 95°C for 1 min, 55°C for 1 min, 72°C for 1 min; (3) one cycles at 72°C for 10 min. The following sets of primers were used for the amplification of SOD-1 cDNA: primers 5′-CTCAGGAGAGCATTCCATCATTG-3′ (upstream) and 5′- ATCACACCAC AAGCCAAGCG-3′ (downstream) designed from the cDNA sequence of Mouse SOD-1 (Bewley, 1998). Glyceraldehyde-3-phosphate dehydrogenase (GAPDH) expression was used as housekeeping gene. Primers for GAPDH were 5′- TTTGTGATGGGTGTGAACCACGAG-3′ (upstream) and 5′-CAACGGATACATTGGGGGTAGGAAC-3′ (downstream; Sabath et al., 1990). The region amplified by PCR of CuZn-SOD was spanned the region between the 375–395 and 501–482, which resulted in a fragment of 129 bp (Bewley, 1998) and 334 for glyceraldehyde-3-phosphate dehydrogenase (GADPH) (Sabath et al., 1990). The PCR products were electrophoresed on 1% agarose gels, stained with ethidium bromide and photographed. To compare the expression of mRNA SOD-1 in MTh cells with M4b cells, the density and area of each band of the SOD-1 PCR products were analyzed with a Scion Image software, and values were normalized to the densitometric values of the corresponding GADPH PCR products.

Immunohistochemistry

Cells were fixed in formaldehyde (4%) in PBS for 30 min and permeabilized in an ascending-descending ethanol battery (50–96%). Protein block was carried out using bovine serum albumin (2%) in PBS and incubation with different primary antibodies according to manufacturer specifications. Antibodies that define patterns of transformation and differentiation of cellular lines were used, such as monoclonal anti-vimentin (1:10, Boehringer Mannheim, Germany) and polyclonal anti-cytokeratin of low molecular weight (prediluted, Biogenex, San Ramon, CA). The presence of neuronal markers was determined using monoclonal antibodies for neuron specific enolase (prediluted, NSE, Biogenex), anti-microtubule associated protein-2 (MAP-2, 1:1,000; Sigma, St. Louis, MO), and anti-synaptophysin (prediluted, Biogenex). Functional neuronal markers were assessed using anti-choline acetyl transferase (ChAT, 1:500; Chemicon, Temecula, CA), monoclonal anti-tyrosine hydroxylase (TH, 1:1,000; Sigma), and polyclonal anti-calcitonin gene related peptide (CGRP, 1:1,000; Sigma). Glial marker antibodies tested included prediluted anti-glial fibrillary acidic protein (GFAP, Biogenex), anti-S-100 (Biogenex) and polyclonal anti-galactocerebroside (1:2,000; Sigma). Labeling was detected using the Labeled Avidin Biotin method (Biogenex), where 20-min incubation times at room temperature were allowed for the secondary antibody, and subsequently similar incubation periods were used for the streptavidin-peroxidase complex. The immunohistochemical reaction was visualized by incubation with 3,3 diaminobenzidine (1 mg/ml, DAKO, Carpintería, CA) in 0.05 M PBS (pH 7.4) and 0.03% H_2O_2 for 5 min at room temperature. The preparation was dehydrated, clarified, and mounted onto synthetic resin for microscopic observation. Negative controls were obtained by omitting the primary antibody, and testing the antibodies mentioned above in the non- neuronal cell line, Hep2 (kind gift, Dr. Lautaro Pérez, Virology Program, ICBM, University of Chile. Data not shown).

Immunoblotting

Cellular proteins were extracted by lysis with a buffer (150 mm NaCl, mm Tris, pH 8; 2 mm EDTA, 1% Triton, and 0.1% sodium dodecylsulfate [SDS]) containing the protease inhibitors phenylmethylsulfonylfluoride (1 mM) and leupeptin (10 mg/ml). The protein content of cells was determined by using the BCA assay (Pierce, Rockford, IL), according to the manufacturer's instructions. Equal amounts (40 mg) of cell extracts were then electrophoresed in an 15% SDS-polyacrylamide gel and electrophoretically transferred to nitrocellulose membranes. Nonspecific binding was blocked with 3% nonfat dried milk in Tris-buffered saline for 2–3 hr at room temperature. To detect cellular ChAT, blots were incubated with a polyclonal anti-choline acetyltransferase antibody (Chemicon, diluted 1:750) overnight at 4°C. Bound antibody was detected using a secondary antibody labeled with horseradish peroxidase (Pierce), followed by development with diaminobenzidine (DAB).

Intracellular Ca^{2+} Measurements

Variations in intracellular Ca^{2+} levels ($[Ca^{2+}]_i$) were assessed by microfluorometry with Indo-1. The cells were incubated at 37°C for 40–60 min with the indicator. Then, coverslips were mounted in a perfusion chamber placed on the stage of a fluorescence inverted microscope (Diaphot-200, Nikon Corp., Tokyo, Japan) equipped with two dichroic mirrors. One dichroic mirror was used to send the excitation light (355 nm) to the cells and the fluorescent light emitted by Indo-1 inside the cells ($>$ 400 nm) to the second mirror. The second dichroic mirror was used to split the fluorescent light into beams of light centered at 410 and 485 nm, respectively. The intensity of light at each wavelength was continuously measured using two photomultipliers, and the analog signal digitized using an A/D converter board (Labmaster, Scientific Solutions, Mentor, OH; Micron Systems, West Friendship, MD) installed in a dedicated PC compatible computer. Digital data was captured and stored in the hard disk for later analysis. A computer program calculated the F_{410}/F_{485} ratio and yielded the corresponding $[Ca^{2+}]_i$ from a calibration curve obtained from a calcium calibration buffer kit (Molecular Probes, Inc., Eugene, OR).

Neurotransmitter agonists were applied externally by a custom-made perfusion system. For analysis of Ca^{2+} signal amplitudes, records were measured from the baseline prior to the stimuli, up to the peak of the response. For analysis of the decay of the response, experimental curves were fitted to a single exponential by the least square fit method.

The compositions of the normal extracellular solutions were (in mM): 135 or 145 NaCl, 5 KCl, 2 $MgCl_2$, 1.5 or 2.5 $CaCl_2$, 10 4-(2-hidroxyethil) piperazine-1-ethanesulfonic acid (HEPES)-NaOH, 10 Dextrose (pH 7.4).

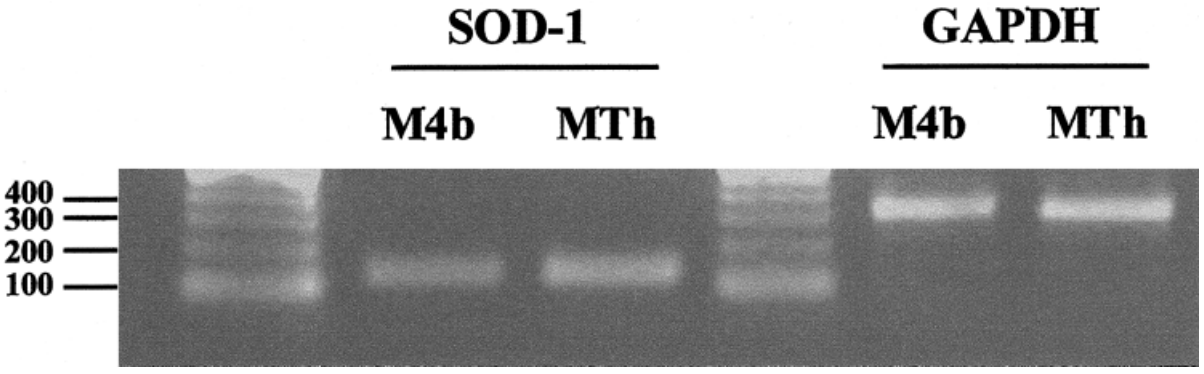

Fig. 1. MTh cells overexpress Cu/Zn superoxide dismutase (SOD-1). Reverse transcriptase-polymerase chain reaction (RT-PCR) assay of mRNA levels corresponding to SOD-1 in M4b and MTh cells. GADPH was routinely performed in parallel. Aliquots (20 μl) of each PCR reaction were run on 1.5% agarose gels and stained with ethidium bromide to visualize the SOD-1 (129 bp) and GAPDH (334 bp) bands. MTh overexpression was estimated as 1.55 of that observed in M4b cells.

[^{3}H]-Choline Uptake Experiments

Approximately 24 hr prior to experiments, cultures were placed in 1 ml serum-free, phenol red free DME/Ham-F_{12} medium. At the time of experiment, 1 μCi [^{3}H]-choline (Sp. Activity ~50 mCi/mmol; Dupont NEN, Wilmington, DE; total volume = 10 μl) was added to each dish and uptake assessed at 1, 3, and 5 min incubation periods (final choline concentration ~0.013 μM). At the end of the uptake period, extracellular solution medium was removed and 50 μl was collected to determine the extracellular fraction. The cells were then rapidly washed 4× with 1 ml cold (4°C) Hank's solution (0.185 g/L $CaCl_2$, 0.09767 g/L $MgSO_4$, 0.4 g/L KCl, 0.06 g/L K_3PO_4, 8.0 g/L NaCl, 0.04788 g/L Na_2PO_4, and 1.0 g/L glucose) to remove nonselectively bound [^{3}H]-choline. Cell membranes were disrupted with 1 ml of 0.1% SDS, and 900 μl of the cell/SDS extract was removed. Ten ml Econo 2 scintillation fluid was added to each vial and vials were analyzed for [^{3}H] content by liquid scintillation counting. The remaining 100 μl was used for protein determination (BCA, Pierce). The amount of [^{3}H]-choline taken up into cells (dpm/mg cell protein) was determined at each time point for each well and normalized to the extracellular [^{3}H]-choline concentration (dpm/ml). Choline uptake (nmol/mg protein/min) was calculated as:

$$U^3H\text{-}C = [IC\ (dpm)/0.9]/[EC\ (dpm)/0.05]/mg\ Prot. \quad (1)$$

where U ^{3}H-C is the [^{3}H]-choline uptake (or distribution volume), IC is the intracellular fraction, EC is the extracellular fraction, 0.9 is the aliquot factor for the intracellular fraction, 0.05 is the aliquot factor for the extracellular fraction, and mg Prot. is the protein content per dish. Transfer coefficients (K_{in}) were determined from the choline uptake versus time data obtained in these experiments from the slope of this uptake curve.

Acetylcholine Release Experiments

For fractional acetylcholine release experiments, cells were incubated for 30 min with 1 μCi [^{3}H]-choline, followed by 4× washes with 1 ml Hank's solution at 37°C (Fiedler et al., 1994; Kotas and Prince, 1987). To induce release, the cells were stimulated with 50 mM K^+, 200 μM glutamate and 100 μM nicotine (Fiedler et al., 1994; Cárdenas et al., 1999). To account for the basal efflux of fractional acetylcholine, determined as tritium release (Kotas and Prince, 1987), samples of the extracellular fluid were taken at 3, 6, 9, and 10 min and their radioactivity was determined. Stimulation was carried out at 11 min, and the average basal efflux was subtracted from the total values of radioactivity to determine the specific, active release (Fiedler et al., 1994). Later, the cells were lysed with 0.1% SDS to determine the intracellular fraction of acetylcholine.

Statistics

Statistical significance was assessed using analysis of variance (ANOVA) and Student's *t*- test. Significance was accepted at the $P < 0.05$ significance level.

RESULTS

MTh Cell Overexpress SOD-1, Whose Gene is Present in Chromosome 16

In order to ascertain the trisomic phenotype, RT-PCR studies were performed to determine overexpression of SOD-1, an enzyme present in mouse chromosome 16 and human autosome 21 (Ault et al., 1989b; Epstein, 1986). Pixel density and area analysis of the bands presented in Figure 1, reveal an expression ratio of 1.55 ± 0.08 of MTh vs. M4b cells (n = 3, $P > 0.01$), suggesting that the trisomic derived line has retained the excess gene dosage inherent to the aneuploid condition.

The Morphology of Differentiated M4b and MTh Cells Indicates the Presence of Neuronal Traits

Both cell lines proliferate readily in standard growth medium, with approximate doubling times of 14 hr. By immunohistochemistry, M4b and MTh cells exhibited the transformation marker vimentin with a labeling pattern of intermediate filament. Low molecular weight cytokeratin

labeling was diffuse and near background levels (data not shown). The presence of neuronal markers was evaluated by the presence of neuronal proteins such as NSE, which showed a cytoplasmic and finely granular staining pattern (Fig. 2A,B). Labeling of another neuronal marker, synaptophysin, was preferentially intense in cells that exhibited morphological differentiated features (long, numerous processes). The pattern of labeling was granular, perinuclear, and also present in the cell processes (Fig. 2C,D). MAP-2 labeling was positive in both cell lines with fibrillary staining surrounding the nucleus and vesicular cytoplasmic structures (data not shown).

Functional markers such as ChAT and CGRP were also evaluated. ChAT staining was cytoplasmic and highly positive in both lines, but no qualitative differences were found when comparing normal and trisomic cells (Fig. 2E,F). Considering the importance of adequately determining the cholinergic phenotype, Western blot analysis were performed (Fig. 2, inset). The study demonstrates the presence of two bands at 66 and 60 kD, with a 60% and 65% reduction in the expression of both bands, respectively, in MTh compared to M4b cells. This finding agrees with our previous studies in cerebral cortex derived lines (Allen et al., 2000), and with molecular weights of various ChAT isoforms (Misawa et al., 1992; Kengaku et al., 1993).

CGRP was also positive, but the intensity and localization of the staining was different for the cell types. The M4b cells exhibited a diminution of labeling when compared to MTh cells, and was preferentially perinuclear, demonstrating no labeling of cellular processes (Fig. 2G). Labeling in MTh cells was homogeneously distributed in the cytoplasm (Fig. 2H). The glial marker S-100 was negative in both cell lines (Fig. 2I, J), as well as GFAP (data not shown), with staining patterns similar to negative controls.

Intracellular Ca^{2+} Signals in M4b and MTh Cell Lines

The response of intracellular Ca^{2+} to specific central neurotransmitter agonists provides proof of central neuronal function at the membrane level, such as the presence of specific and functional receptors which confer excitability properties (i.e., glutamatergic receptors) (Kandel and Siegelbaum, 2000). Since it is known that Matrigel promotes cellular differentiation (Lin and Bissel, 1993; Streuli, 1999) and increases the sensitivity to different neurotransmitter agonists in neuronal cell lines derived from normal and trisomy 16 fetal mice (Cárdenas et al., 1999), we evaluated the Ca^{2+} responses induced by glutamate and nicotine in M4b and MTh cells grown in Matrigel. In these experiments, cells were kept in culture in Matrigel for 3 or 4 days.

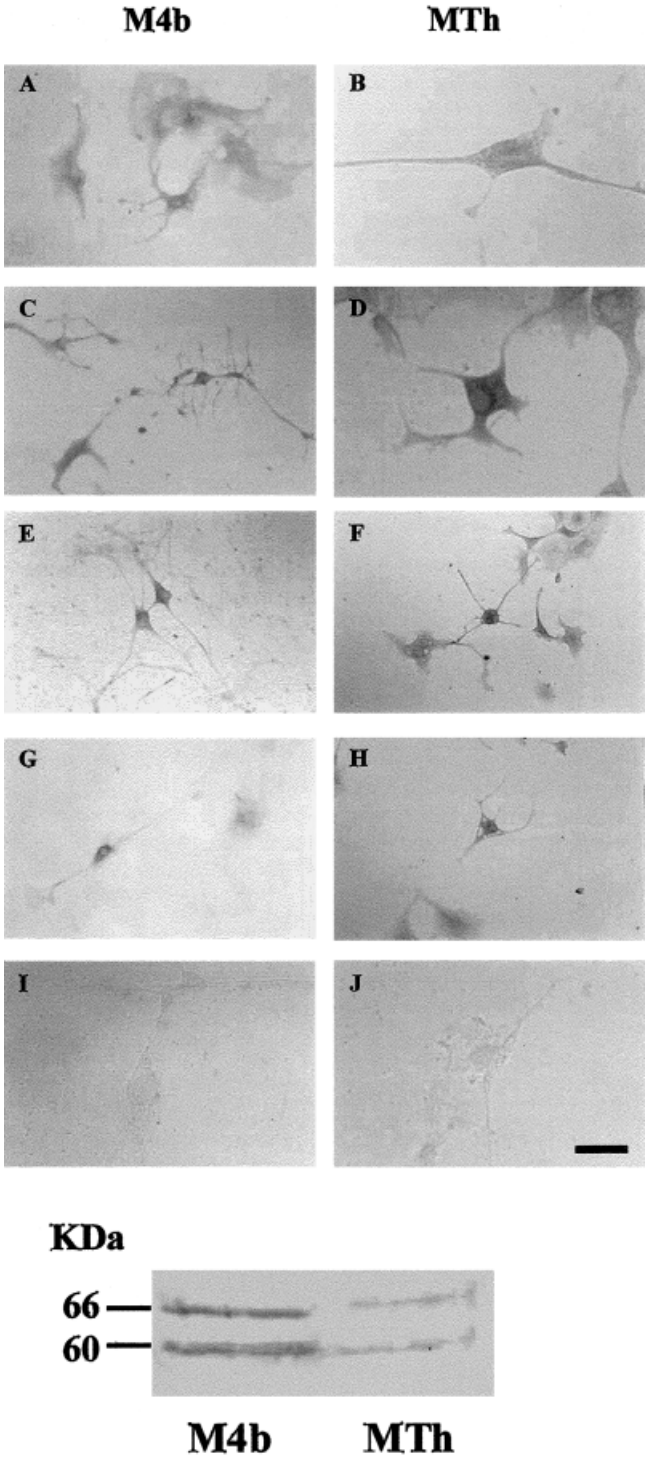

Fig. 2. Cell lines derived from spinal cord of normal and trisomy 16 mouse fetuses present neuronal markers. Immunohistochemistry procedures were carried out according to Materials and Methods. Positive labeling for neuron specific enolase (NSE; **A,B**), synaptophysin (**C,D**), choline acetyl transferase (ChAT; **E,F**), and calcitonin gene related peptide (CGRP; **G,H**) is present in the normal (M4b) and trisomic (MTh) cell lines. Glial markers such as S-100 (**I, J**) are negative. Scale bar = 25 μm for B,D,I,J; 100 μm for A,C,E,F,G,H). The **inset** (lower center) presents the Western blot study for ChAT in both cell lines, indicating a lower expression of the enzyme in MTh cells, compared to M4b.

TABLE I. Amplitude of $[Ca^{2+}]_i$ Responses to the Different Agonists in M4b and MTh Indo-1-Loaded Cells†

	Amplitude of $[Ca^{2+}]_i$ (nM)			
Agonist	M4b	n	MTh	n
Glutamate	596 ± 53	12	553 ± 45	11
NMDA[a]	600 ± 33	14	684 ± 97	19
Kainate	405 ± 30	7	534 ± 69	16
Nicotine	412 ± 19	39	492 ± 26★	40
Noradrenaline	465 ± 52	29	475 ± 43	27

†Amplitude values correspond to the maximum value of $[Ca^{2+}]_i$ after the application of the each agonist. Data represent means ± S.D.
★$P < 0.05$ compared with M4b cells.
[a]NMDA, N-methyl-D-aspartate.

TABLE II. Time Constant (τ) of the Decay Phase of $[Ca^{2+}]_i$ Responses to the Different Agonists in M4b and MTh Indo-1-Loaded Cells†

	τ (sec)			
Agonist	M4b	n	MTh	n
Glutamate	36 ± 6	12	13 ± 3★	9
NMDA[a]	25 ± 4	14	16 ± 13	19
Kainate	21 ± 3	7	14 ± 6	13
Nicotine	47 ± 6	24	36 ± 6	30
Noradrenaline	27 ± 4	9	26 ± 5	15

†Time constant (τ) values result from exponential fits of the decay phase of $[Ca^{2+}]_i$ responses, using the least square method. Data represent means ± S.D. of cells with single exponential decays.
★$P < 0.05$ compared with M4b cells.
[a]NMDA, N-methyl-D-aspartate.

Basal $[Ca^{2+}]_i$ in cells cultured in Matrigel was significantly greater in the trisomic cells compared to the normal cell line ($P < 0.05$); 112 ± 4 (n = 95) for M4b and 129 ± 7 (n = 95) for MTh cells.

M4b and MTh cell lines respond to glutamatergic receptor agonists. Approximately 15% of M4b and 60% of MTh cells, cultured on Matrigel, responded to glutamate (100–200 μM) with a rapid and transient increase in $[Ca^{2+}]_i$. Table I shows the amplitude of the response to this agonist in M4b and MTh cells. Analysis of the decay in the $[Ca^{2+}]_i$ responses to glutamate, showed that 100% of M4b cells (n = 12) display a single exponential kinetics for the decay, while 82% of MTh cells (n = 9) exhibit a single exponential kinetics and 18% exhibited two components in the decay phase. Time constant values of the decay responses with single exponential kinetics were significantly different ($P < 0.05$) between both cell types, with time constants of 36 ± 6.8 sec (n = 12) and 13 ± 3 sec (n = 9) for M4b and MTh cells, respectively (Table II).

To study the dependence of extracellular Ca^{2+} in these responses, we stimulated M4b and MTh cells with glutamate in Ca^{2+} free external solution (Ca^{2+}-free medium plus 5 mM EGTA). Over 70% of M4b and MTh cells respond to glutamate both in the presence and absence of extracellular Ca^{2+}(Ca^{2+}-free medium plus 5 mM EGTA). Figure 3A shows typical records in the aforementioned conditions, suggesting the existence of either ionotropic and metabotropic glutamate receptors. To further clarify whether the latter responses were due to activation of metabotropic receptors, we stimulated the cells with 100 μM ACPD, a known specific metabotropic glutamate receptor agonist. In the latter case, we also observed a $[Ca^{2+}]_i$ rise in M4b and MTh cell.

To characterize the ionotropic glutamate activity, we evaluated the effect of N-methyl-D-aspartate (NMDA), AMPA, and kainate on $[Ca^{2+}]_i$ signals. As shown in Figure 4A, NMDA (100–200 μM) induced an increase in $[Ca^{2+}]_i$ in both cell lines. We estimated that 22% of M4b (n = 10) and 61% of MTh cells (n = 11) exhibited such behavior. The rise of $[Ca^{2+}]_i$ induced by NMDA was completely inhibited by the selective NMDA receptor antagonist AP_5 (70–100 μM).

Kainate (100–200 μM) also induced an increase of $[Ca^{2+}]_i$ both M4b and MTh cells. The rise of $[Ca^{2+}]_i$ induced by kainate was inhibited by the AMPA/kainate receptor antagonist NBQX (80–100 μM), as shown in Figure 4B. We observed that 23% of M4b (n = 13) and 76% of MTh (n = 10) respond to kainate, but neither M4b nor MTh cells respond to AMPA (100–200 μM).

Table I shows the amplitude of the $[Ca^{2+}]_i$ response of M4b and MTh cells to the ionotropic glutamatergic agonists. In Table II is shown time constant values of the single decay responses induced by NMDA or kainate. Almost 100% of the M4b and MTh respond to NMDA or kainate with single exponential kinetics for the decay. Nonsignificant differences in the amplitude and decay responses induced by NMDA and kainate between both cell types were observed.

M4b and MTh cell lines respond to nicotine and noradrenaline. Approximately 50% of M4b and 60% MTh cells, cultured on Matrigel, responded to nicotine (100–200 μM), with a rapid and transient increase in $[Ca^{2+}]_i$ .However, muscarine did not induce a rise of $[Ca^{2+}]_i$ in both types of cells. The effect of nicotine on $[Ca^{2+}]_i$ was reversibly inhibited by 100 μM dihydro-β-erythroidine, a competitive nicotinic receptor antagonist (Fig. 5A). As shown in Table I, the amplitude of the nicotine responses in MTh cells was significantly greater in the trisomic cells compared to normal cell line ($P < 0.05$), 412 ± 19 (n = 39) for M4b and 492 ± 26 (n = 40) for MTh (Table I). Analysis of the decay in the $[Ca^{2+}]_i$ responses to nicotine, showed that 62% of M4b cells (n = 24) and 75% of MTh cells (n = 30) display a single exponential kinetics for the decay; 38% of M4b cells (n = 15) and 25% of MTh cells (n = 10) exhibited two components in the decay phase. We observed no significant differences in time constant values of the decay responses induced by nicotine (Table II).

Finally, we evaluated the sensitivity of M4b and MTh cells to noradrenaline. 40% of M4b (n = 29) and 60% of MTh cells (n = 27) respond to noradrenaline (50–150 μM) with transient increases of $[Ca^{2+}]_i$. The

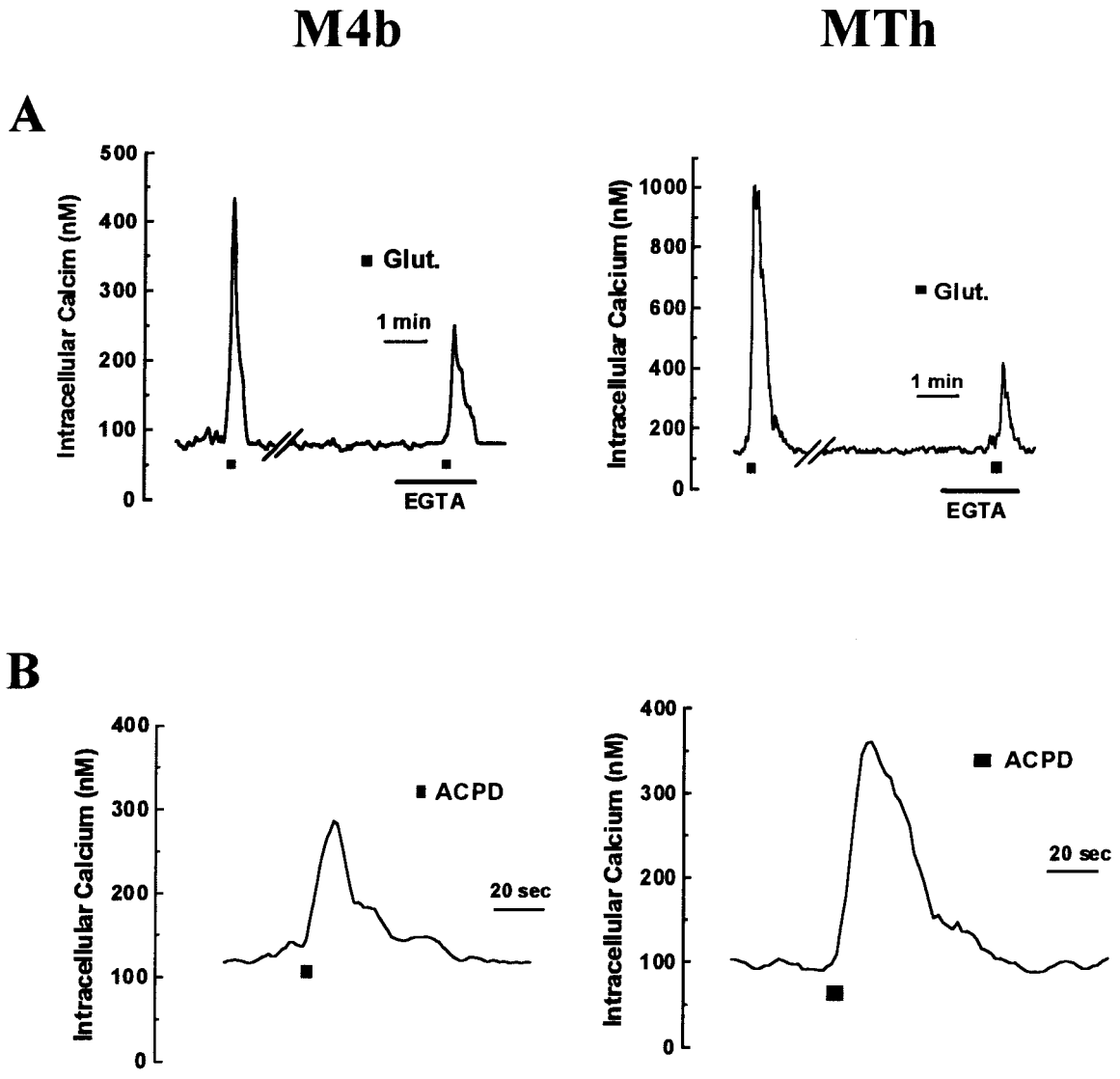

Fig. 3. Glutamate and ACDP induces increase $[Ca^{2+}]_i$ in M4b and MTh cells. **A:** Indo-1 loaded M4b or MTh cells were stimulated for 10 sec with 150 μM glutamate (indicated by filled boxes), in the presence or absence of extracellular Ca^{2+} (Ca^{2+}-free medium plus 5 mM EGTA indicated by the horizontal lines labeled EGTA at the bottom of the figure). **B:** ACPD (100 μM, filled boxes) applied externally for 10 sec induced increases in intracellular Ca^{2+} in M4b and MTh cells. These experiments are representative of four carried out in M4b or MTh cells.

effect of noradrenaline on $[Ca^{2+}]_i$ was reversibly inhibited by 100 μM benoxathian, a selective α_1 adrenoreceptor antagonist (Fig. 5B). The amplitude of the $[Ca^{2+}]_i$ response of M4b and MTh cells to noradrenaline is shown in Table I. In Table II is shown time constant values of the single decay responses; 44% of M4b cells (n = 19) and 55% of MTh cells (n = 15) display a single exponential kinetics for the decay; 56% of M4b cells (n = 10) and 45% of MTh cells (n = 12) exhibited two components in the decay phase. Nonsignificant differences in the responses induced by noradrenaline were observed (Tables I and II).

[^{3}H]-Choline Uptake Into M4b and MTh Cells

As cholinergic dysfunction has been demonstrated in primary trisomy 16 spinal cord tissue cultures (Fiedler et al., 1994) and M4b and MTh cells lines exhibit positive immunoreactivity to the choline acetyl transferase antibody, we compared the [^{3}H]-choline incorporation and ACh release between these cells.

Coline incorporation was evaluated in the spinal cord cell lines at incubation periods of 1, 3, and 5 min with 1 μCi [^{3}H]-choline. Figure 6A shows that although MTh cells exhibited a tendency toward higher uptake values

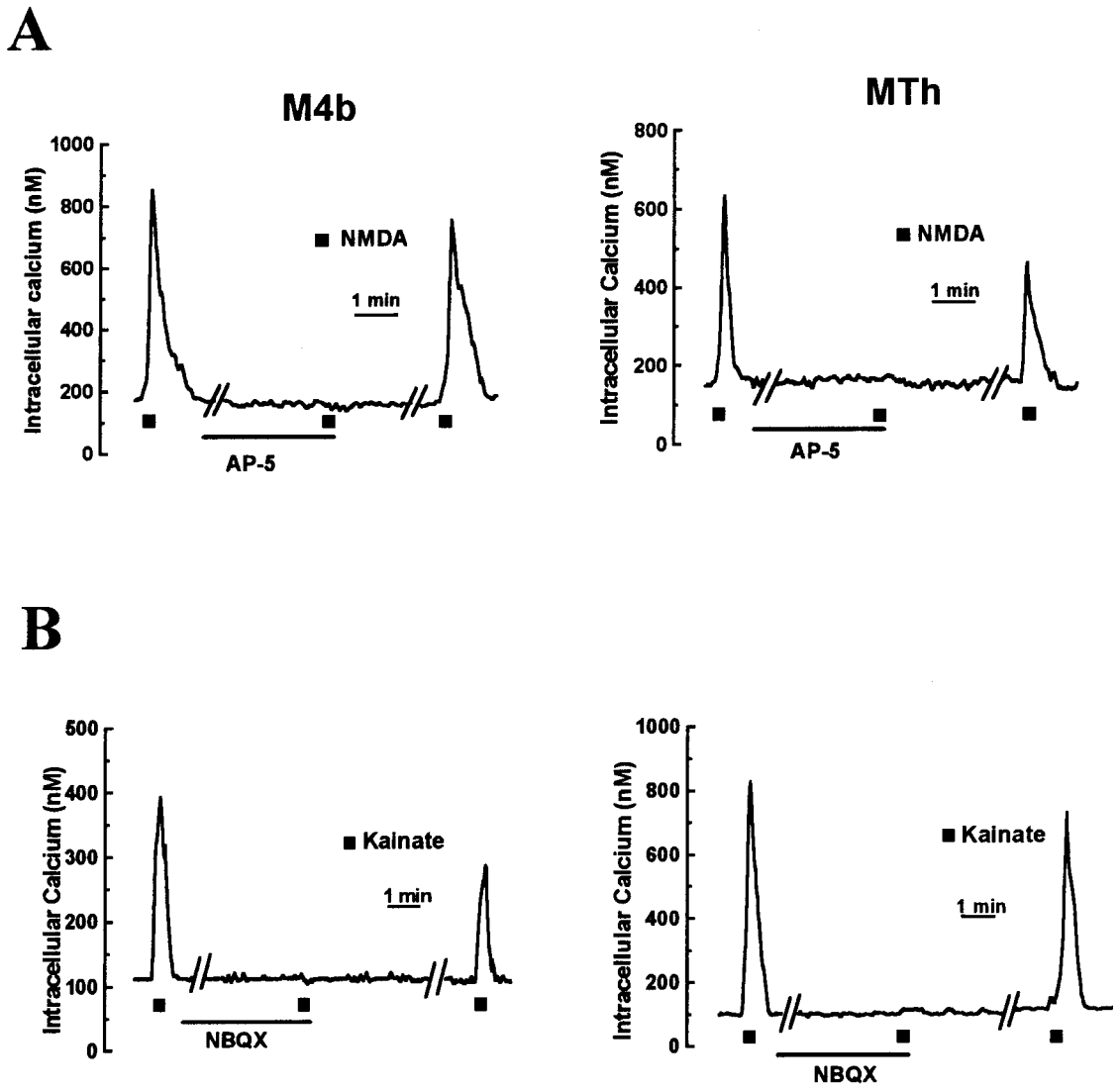

Fig. 4. Ionotropic glutamate receptor agonists produce $[Ca^{2+}]_i$ rises in M4b and MTh cells. Indo-1 loaded M4b or MTh cells were stimulated for 10 sec with 150 μM N-methyl-D-aspartate (NMDA; **A**) or 150 μM kainate (**B**) in the absence or presence of 90 μM AP_5 or 90 μM NBQX added during the time periods indicated by the horizontal lines at the bottom of the figure. These experiments are representative of four carried out in M4b or MTh cells.

than controls, no significant difference in choline uptake exists between cell types at the incubation periods studied. The rate of uptake (ml/mg/min) for both cell lines was determined by linear regression of the slopes of uptake values at their corresponding incubation periods. The choline uptake rates were 0.016 ml/mg/min and 0.022 ml/mg/min for M4b and MTh, respectively.

To determine the transport system by which choline enters the cell, we evaluated the effect of 10 μM hemicholinium-3, a potent inhibitor of the high-affinity choline uptake system. Neither M4b nor MTh cells showed significant sensitivity to hemicholinium-3. In the M4b cell line, uptake after incubation with hemicholinium-3 was 0.010 ± 0.0024 ml/mg/min (n = 3) compared to a control uptake value of 0.018 ± 0.004 ml/mg/min (n = 3). In the MTh line, uptake after incubation with hemicholinium-3 was 0.041 ± 0.005 ml/mg/min (n = 3) compared to a control uptake value of 0.043 ± 0.016 ml/mg/min (n = 3).

Also, choline uptake was assessed after 1 min incubation with 1, 5, 10, 50, and 100 μM solutions of cold choline to evaluate saturable choline uptake. Inverse uptake values were plotted versus concentration and the data fitted to obtain Michaelis-Menten curves from which V_{max} and K_m values were assessed. V_{max} and K_m values of 0.0083 ml/mg/min and 0.04 was

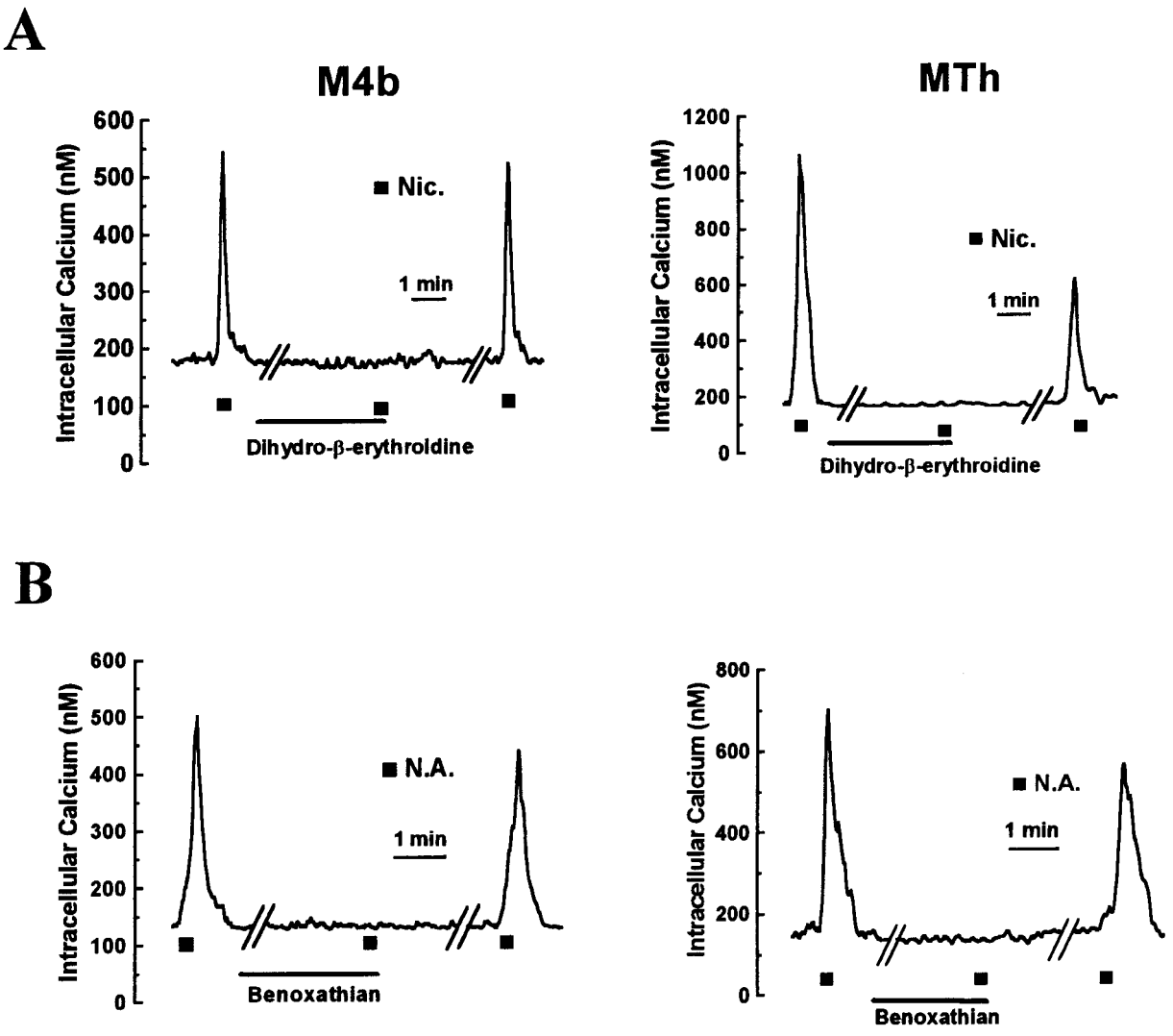

Fig. 5. Nicotine (Nic.) and noradrenaline (N.A.) increase the $[Ca^{2+}]_i$ in M4b and MTh cells. Indo-1 loaded M4b or MTh cells were stimulated for 10 sec with 150 μM nicotine (**A**) or 100 μM noradrenaline (**B**) in the absence or presence of 100 μM dihydro-β-erythroidine or 100 μM benoxathian added during the time periods indicated by the horizontal lines at the bottom of the figure. These experiments are representative of four carried out in M4b or MTh cells.

measured for the M4b cell line. The MTh cells exhibited a V_{max} of 0.016 ml/mg/min and K_m of 0.063.There were no differences for these kinetic parameters for the cell lines (Fig. 6B).

Fractional Release of Acetylcholine Upon Stimulation

For fractional ACh release experiments, cells were stimulated for 1 min with 50 mM external K^+, 200 μM glutamate or 100 μM nicotine. As shown in Figure 7, the fractional release of acetylcholine induced by K^+, glutamate or nicotine was significantly higher in MTh cells. Depolarization induced by 50 mM external K^+ increased by 9-fold the fractional release of tritium in MTh cells, compared to M4b ($n = 5$, $P < 0.01$), while glutamate and nicotine increased the fractional release 4-fold of MTh cells ($P < 0.05$).

DISCUSSION

In the present work, we studied the presence of neuronal markers and the response of $[Ca^{2+}]_i$ to spinal cord receptors agonists in permanent cell lines derived from the spinal cord of normal and trisomy 16 fetal mice. Interestingly, the trisomic condition appears preserved in the MTh line, in light of our studies using RT-PCR studies of SOD-1 expression. Such studies suggest that the trisomic condition is present, and that it results in the rate of overexpression expected by gene dosage.

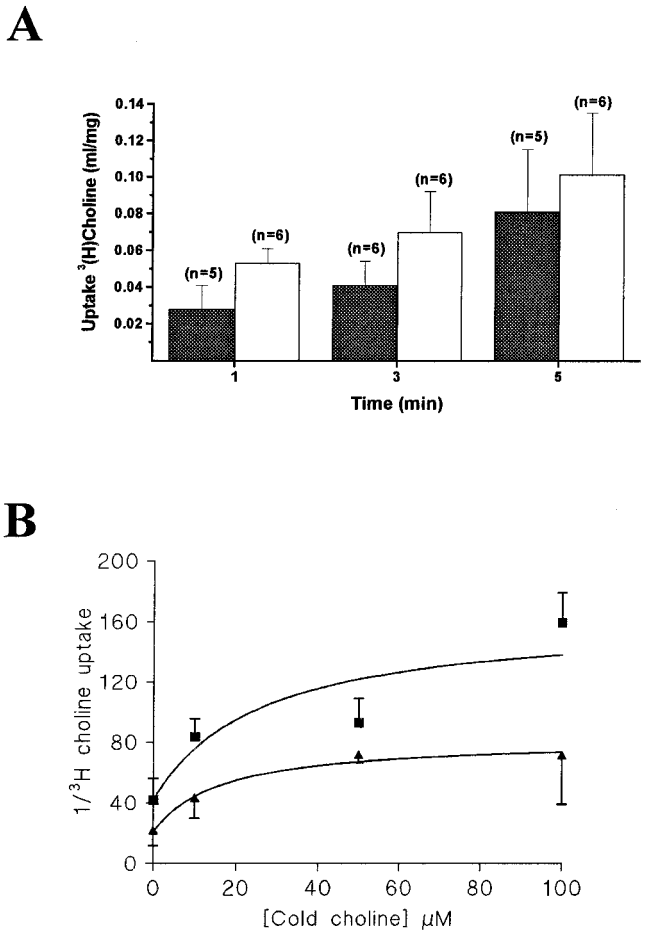

Fig. 6. ^{3}[H]-choline incorporation in M4b and MTh cells. **A:** Incorporation of ^{3}[H]-choline at incubation periods of 1, 3, and 5 min with 1 μCi tritiated choline. Choline uptake is expressed as ml/mg/min. M4b values are represented by black bars and MTh are represented by white bars. **B:** Saturation of choline uptake (as 1 μCi ^{3}[H]-choline) in the presence of increasing concentrations of unlabeled choline (cold choline). M4b values are represented by squares and MTh are represented by triangles. Data represent average uptake ± S.E of the number of experiments shown in parenthesis. No significant differences were observed between the two cell types.

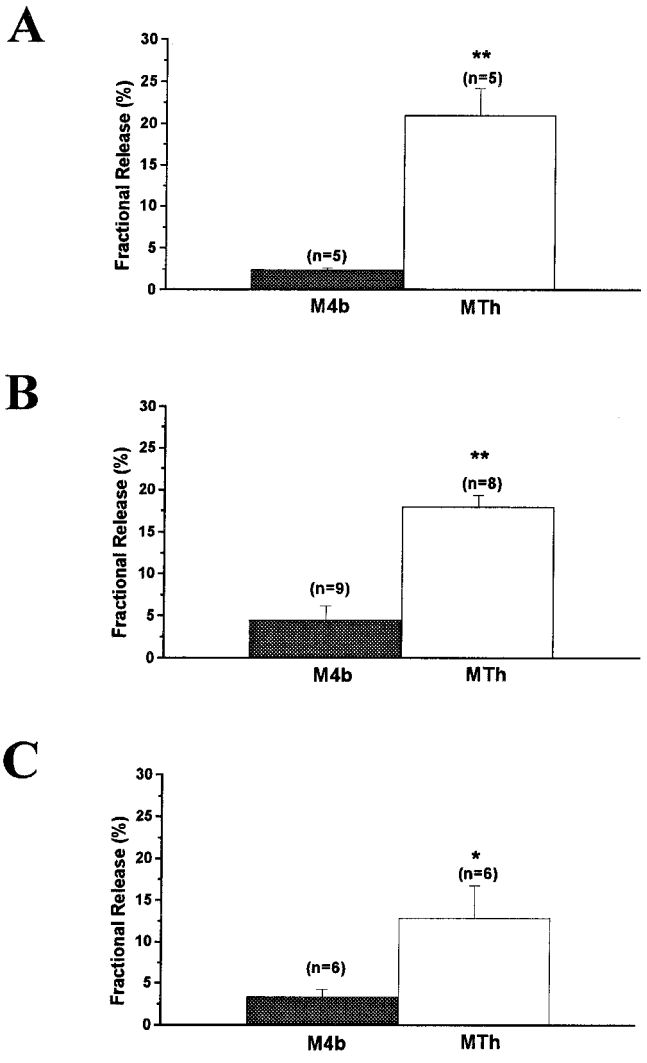

Fig. 7. Fractional release of acetylcholine induced by K^+, glutamate, and nicotine. Release of acetylcholine (Kotas and Prince, 1987) was measured in previously ^{3}[H]-choline loaded M4b (black bars) and MTh (white bars) cells, after incubation for 1 min with 50 mM K^+ (**A**), 200 μM glutamate (**B**), or 100 μM nicotine (**C**). Values represent mean fractional release ± S.E. of the number of experiments shown in parenthesis. $\star P < 0.01$, $\star\star P < 0.05$ compared MTh with M4b cells.

The presence of neuronal markers by immunohistochemistry is clear, and the neuronal lineage is further demonstrated by the absence of glial markers. Further, Western blot analysis for ChAT evidenced two bands at 66 and 60 kD, which may correspond to variants due to alternative splicing, which reportedly determines up to seven different forms in rat and mouse spinal cords (Misawa et al., 1992; Kengaku et al., 1993). Interestingly, we observed a reduction in the expression of both forms in the MTh cell line with regards to M4b. These findings closely resemble those of previously established cell lines from nervous tissue, using our UCHT1 conditioned medium. Indeed, our normal and trisomy 16 cerebral cortex derived lines show a similar labeling pattern indicating a neuronal origin and reduced ChAT expression (Cárdenas et al. 1999; Allen et al., 2000). Our experience with other cell lines so established from other brain regions is similar (Arriagada et al., 2000; Dagnino-Subiabre et al., 2000), demonstrating that our transformation protocol is primarily effective in immortalizing neuronal tissue.

Intracellular Ca^{2+} homeostasis is critical in cell function, and affects the critical neuronal function of neurotransmitter secretion. We therefore proceeded to study the response of $[Ca^{2+}]_i$ to several neurotransmitter agonists and thus evaluate the presence of functional receptors. Considering also that our cell lines express a predominant cholinergic phenotype in light of their positive ChAT

staining and Western blot analysis, we complemented these studies by evaluating cholinergic function via uptake of [^{3}H]-choline and release after stimulation. Our results showed that basal $[Ca^{2+}]_i$ levels were significantly greater in MTh cell compared to M4b, suggesting alterations in the intracellular Ca^{2+} homeostasis in the trisomic cells. These findings agree with those previously reported by Schuchmann et al. (1998), who observed the same differences in primary cultures of hippocampal neurons from normal and trisomy 16 fetuses. Also, we had previously reported greater basal $[Ca^{2+}]_i$ levels in neuronal cell lines derived from the cerebral cortex trisomy 16 mice (CTb) compared to their normal derived counterparts (Cárdenas et al., 1999). These findings suggest that impairments in intracellular Ca^{2+} buffering may be a generalized feature in the trisomic condition, a situation that could determine profound impairments in neuronal function.

Both M4b and MTh cells respond with a rapid and transient $[Ca^{2+}]_i$ signal to cholinergic, glutamatergic and adrenergic receptor agonists. We also conclude that both ionotropic and metabotropic receptors are present in these cell lines, in light of responsiveness to the ionotropic receptor agonists (NMDA and kainate), and to glutamate in absence of extracellular Ca^{2+} and stimulated by ACPD. Ionotropic and metabotropic receptors are present in spinal neurons (Fundytus et al., 2001; Dingledine and McBain, 1999), and the increase in $[Ca^{2+}]_i$ in response to metabotropic stimuli indicates the presence of type I metabotropic receptors in our cell lines, which reportedly exist in spinal neurons (Fundytus et al., 2001). The latter receptors are coupled to Phospholipase-C (PLC), and increase $[Ca^{2+}]_i$ via production of IP_3 and release from intracellular stores (Dingledine and McBain, 1999). We also observed that lesser number of M4b cells respond to the different agonists, since this difference is more dramatic in the glutamatergic responses, where approximately 20% of normal cells respond to glutamate versus 60% of trisomic cells. At present, possible explanations for this finding are: (1) a greater excitability, due to increased expression of a glutamatergic receptor. Indeed, the kainate subunit GluR5 gene of the glutamate receptor is present in chromosome 16, and its overexpression could alter membrane excitability and yield greater sensitivity to glutamate (Gregor et al., 1994). Furthermore, an overexpression of GluR1 (Arai et al., 1996) and mGluR5 (Oka and Takashima, 1999) receptors has been reported in cerebral cortex of Down syndrome patients. In turn, this may have consequences in other ionic conductances, which reportedly are altered in trisomy 16 spinal cord neurons (Orozco et al., 1987); (2) different populations of neurons in the trisomic cells are more sensitive to differentiation. We acknowledge the possibility the transformation method may have targeted different populations of neurons in the normal and trisomic cultures. However, there is also evidence that the trisomic condition may result in enhanced sensitivity to stimuli. The gene that encodes for the α and β interferon receptor is also in murine chromosome 16 (Epstein, 1986), and its overexpression could lead to changes in the cells that favor arrest in proliferation and differentiation (Hwang et al., 1995), and therefore a greater sensitivity to neurotransmitter stimuli in the trisomic condition.

The amplitude of $[Ca^{2+}]_i$ responses to nicotine were greater in the trisomic cells compared to the normal cell line. This is comparable to results previously reported by our group (Cárdenas et al., 1999), where we observed that the amplitude of the $[Ca^{2+}]_i$ responses to nicotine was greater in the CTb cell line from cerebral cortex of trisomy 16 mice, compared to its normal derived counterpart CNh.

Analysis of the exponential decay responses to glutamate demonstrates the presence of faster time- dependent kinetics for MTh cells compared to normal cells. It has been observed that neurons from other areas of the nervous system of trisomic mice exhibit slower decays (Schuchmann et al., 1998; Cárdenas et al., 1999). Further, trisomy 16 hippocampal neurons possess slower depolarization and repolarization rates than control (Galdzicki et al., 1993). However, electrophysiological data clearly demonstrate faster kinetics in the action potentials of trisomy 16 spinal cord (Orozco et al., 1987) and dorsal root ganglia (DRG) neurons (Caviedes et al., 1990). Further, Na^+ currents in murine trisomy 16 and K^+ currents in human trisomy 21 DRG neurons (Nieminen et al., 1988; Caviedes et al., 1990) show accelerated kinetics. It is tempting to speculate that the trisomic condition affects different areas of the central nervous system in a differential fashion (Fiedler et al., 1994), and that the spinal cord would be a region that tends to exhibit faster kinetics in membrane-related electrical phenomenon. This is further supported by our analysis of the exponential decay of the responses to glutamate, which demonstrates the presence of faster time dependent kinetics for MTh cells compared to normal cells. The consequential shorter periods of activation could be related to overall depressed responsiveness to nociceptive stimulation reported by Martínez-Cu´e et al. (1999).

Our studies of cholinergic function on our two cell lines revealed no significant differences in choline uptake between trisomic and normal cells (Fig. 6). However, we previously observed lower choline uptake in neurons in primary cultures of trisomy 16 spinal cord compared with neurons of matched controls (Fiedler et al., 1994). Also, we observed lower choline uptake in the trisomic cortical cell lines CTb (Allen et al., 2000). We are unclear at present regarding this finding, which could be due to lack of differentiation, a possibility currently under investigation. The fact that this uptake was not affected by hemicholinium-3 may indicate that culture conditions may need supplementing in order to induce the expression of this transport system (Williams and Rylett, 1990). Interestingly, we observed significantly increased acetylcholine release in MTh compared to M4b cells (Fig. 7). This does not agree with previous results by our group in cortical cell lines (Allen et al., 2000), where the trisomic condition evidenced a reduced release of the neurotransmitter in response to stimulation. We must acknowledge,

however, that the increased release in MTh cells appears paralleled by a greater the number of cells responding to glutamate or nicotine with increased $[Ca^{2+}]_i$. We therefore acknowledge the possibility that an increased number of responsive cells in the MTh line may underlie enhanced neurotransmitter release.

Interestingly, Martínez-Cué et al. (1999), using Ts65Dn mice, showed a faster escape response than controls in the hot plate test, but total licking behavior was reduced in the aneuploid condition. A plausible explanation may lie in the fact that the hot plate test relates to local reflex motor activity where cortical control is less evident, whereas licking behavior would necessarily imply perception and conscience of pain, thus involving cortical areas. As previously mentioned, trisomic spinal cord and dorsal root ganglia (Scott et al., 1983; Caviedes et al., 1990) exhibit greater electrical excitability which could relate to enhanced neurotransmitter release. Conversely, trisomic cerebral neurons in culture, as well as our trisomic cortical cell lines, express decreased acetylcholine release (Fiedler et al., 1994; Allen et al., 2000), which supports the notion that licking behavior may be impaired due to depressed cerebral cortex activity.

Down's syndrome is a condition where gene overexpression is the commanding feature. The discovery of the effects of excess gene dosage and their interactions is essential for therapy. Cellular models are then necessary to study these phenomena at the cellular and molecular level. In this regard, our cell lines could provide valuable information on neuronal mechanisms underlying nervous system dysfunction in the aneuploid condition.

ACKNOWLEDGMENTS

We acknowledge the technical help of Mr. Fernando Guzmán.

REFERENCES

Acevedo LD, Galdzicki Z, McIntosh AR, Rapoport SI. 1995. Increased inward current in septal neurons from the trisomy 16 mouse, a model for Down's syndrome. Brain Res 701:89–98.

Allen DD, Martín J, Cárdenas AM, Rapoport SI, Caviedes R, Caviedes P. 2000. Impaired cholinergic function in cell lines derived from the cerebral cortex of normal and trisomy 16 mice. Eur J Neurosci 12:3259–3264.

Arai Y, Mizuguchi M, Takashima S. 1996. Excessive glutamate receptor 1 immunoreactivity in adult Down syndrome brains. Pediatr Neurol 15: 203–206.

Arriagada C, Dagnino-Subiabre A, Caviedes P, Martín J, Caviedes R, Segura-Aguilar J. 2000. Studies of aminochrome toxicity in a mouse derived neuronal cell line: is this toxicity mediated via glutamate transmission?. Amino Acids 18:363–373.

Ault B, Caviedes P, Rapoport SI. 1989a. Neurophysiological abnormalities in cultured dorsal root ganglion neurons from the trisomy 16 mouse fetus, a model for Down syndrome. Brain Res 485:165–170.

Ault B, Caviedes P, Hidalgo J, Epstein CJ, Rapoport SI. 1989b. Electrophysiological analysis of cultured fetal mouse dorsal root ganglion neurons transgenic for human superoxide dismutase-1, a gene in the Down syndrome region of chromosome 21. Brain Res 497:191–194.

Bewley GC. 1998. cDNA and deduced amino acid sequence of murine Cu/Zn superoxide dismutase. Nucleic Acids Res 16:2728–2728.

Cárdenas AM, Rodríguez MP, Cortés MP, Alvarez RM, Wei W, Rapoport SI, Shimahara T, Caviedes R, Caviedes P. 1999. Intracellular calcium signals in immortal cell lines derived from the cerebral cortex of normal and trisomy 16 fetal mice, an animal model of human trisomy 21 (Down syndrome). Neuroreport 10:363–369.

Caviedes R, Stanbury JB. 1976. Studies on a cell line from a functional rat thyroid tumor in continuous culture. Endocrinology 99:549–554.

Caviedes P, Ault B, Rapoport SI. 1990. The role of altered sodium currents in action potential abnormalities of cultured dorsal root ganglion neurons from trisomy 21 (Down syndrome) human fetuses. Brain Res 510:229–236.

Caviedes P, Olivares E, Caviedes R, Jaimovich E. 1993. Calcium fluxes, ion currents and dihydropyridine receptors in a newly established cell line from rat heart muscle. J Molec Cell Cardiol 25:829–845.

Caviedes P, Caviedes R, Liberona JL, Jaimovich E. 1994. Ion currents in a skeletal muscle cell line from a Duchenne muscular dystrophy patient. Muscle Nerve 17:1021–1028.

Coyle JT, Oster-Granite ML, Reeves RH, Gearhardt JD. 1988. Down syndrome, Alzheimer's disease and the trisomy 16 mouse. Trends Neurosci 11:390–394.

Dagnino-Subiabre A, Marcelain K, Arriagada C, Paris I, Caviedes P, Caviedes R, Segura-Aguilar J. 2000. Angiotensin receptor II is present in dopaminergic cell line of rat substantia nigra and it is down regulated by aminochrome. Molec Cell Biochem 212:131–134.

Dingledine R, McBain CJ. 1999. Glutamate and aspartate. In: Siegel GJ, editor. Basic neurochemistry. Molecular, cellular and medical aspects. 6th Edition. Philadelphia: Lippincott-Raven.

Epstein CJ. 1986. The neurobiology of Down syndrome. NY: Raven Press. p 1–15.

Epstein CJ, Cox DR, Epstein LB. 1985. Mouse trisomy 16: an animal model of human trisomy 21 (Down syndrome). Ann N Y Acad Sci 450:157–168.

Fiedler J, Rapoport SI, Epstein CJ, Caviedes R, Caviedes P. 1994. Altered cholinergic function in cultured neurons from the trisomy 16 mouse fetus, a model for Down Syndrome. Brain Res 658:27–32.

Fundytus ME, Yashpal K, Chabot JG, Osborne MG, Lefebvre CD, Dray A, Henry JL, Coderre TJ. 2001. Knockdown of spinal metabotropic glutamate receptor 1 (mGluR(1)) alleviates pain and restores opioid efficacy after nerve injury in rats. Br J Pharmacol 132:354–367.

Galdzicki Z, Coan E, Rapoport SI. 1993. Cultured hippocampal neurons from trisomy 16 mouse, a model for Down's syndrome, have an abnormal action potential due to a reduced inward sodium current. Brain Res 604:69–78.

Gregor P, Gaston SM, Yang X, O'Regan JP, Rosen DR, Tanzi RE, Patterson D, Haines JL, Horvitz HR, Uhl GR, Brown RH. 1994. Genetic and physical mapping of the GLUR5 glutamate receptor gene on human chromosome 21. Hum Genet 94:565–570.

Hwang SY, Hertzog PJ, Holland KA, Sumarsono SH, Tymms MJ, Hamilton JA, Whitty G, Bertoncello I, Kola I. 1995. A null mutation in the gene encoding a type I interferon receptor component eliminates antiproliferative and antiviral responses to interferons alpha and beta and alters macrophage responses. Proc Natl Acad Sci USA 92:11284–11288

Kandel ER, Siegelbaum SA. 2000. Synaptic Integration. In: Kandel E, Schwartz J, Jessell T, editors. Principals of neural science, 4th edition. New York: McGraw Hill. p 207–228.

Kengaku M, Misawa H, Deguchi T. 1993. Multiple mRNA species of choline acetyltransferase from rat spinal cord. Brain Res Mol Brain Res 18:71–76.

Kotas A, Prince AK. 1987. High-affinity uptake of choline, a marker for cholinergic nerve terminals, is not specific in developing rat brain. Brain Res 432:175–181.

Liberona JL, Caviedes P, Tascón S, Giglio JR, Sampaio S V, Hidalgo J, Caviedes R, Jaimovich E. 1997. Ion channels during differentiation of a human skeletal muscle cell line. J Muscle Res Cell Motil 18:587–598.

Lin CQ, Bissell MJ. 1993. Multi-faceted regulation of cell differentiation by extracellular matrix. FASEB 7:737–743.

Martínez-Cué C, Baamonde C, Lumbreras MA, Vallina IF, Dierssen M, Flórez JA. 1999. A murine model for Down syndrome shows reduced responsiveness to pain. Neuroreport 10:1119–1122.

Mattson MP, Rydel RE. 1992. β-amyloid precursor protein and Alzheimer's disease: the peptide plot thickens. Neurobiol Aging 13:617–621.

Misawa H, Ishii K, Deguchi, T. 1992. Gene expression of mouse choline acetyltransferase. Alternative splicing and identification of a highly active promoter region. J Biol Chem 267:20392–20392.

Nieminen K, Suárez-Isla B, Rapoport SI. 1988.. Electrical properties of cultured dorsal root ganglion neurons from normal and trisomy 21 human fetal tissue. Brain Res 474:246–254.

Oka A, Takashima S. 1999. The up-regulation of metabotropic glutamate receptor 5 (mGluR5) in Down's syndrome brains. Acta Neuropathol (Berl) 97:275–278.

Orozco CB, Smith SA, Epstein CJ, Rapoport SI. 1987. Electrophysiological properties of cultured dorsal root ganglion and spinal cord neurons of normal and trisomy 16 fetal mice. Brain Res 429:111–122.

Reeves RH, Irving NG, Moran TH, Wohn A, Kitt C, Sisodia SS, Schmidt C, Bronson RT, Davisson MT. 1995. A mouse model for Down syndrome exhibits learning and behaviour deficits. Nature Genet 11:177–183.

Sabath DE, Broome HE, Prystowsky MB. 1990. Glyceraldehyde-3-phosphate dehydrogenase mRNA is a major interleukin 2-induced transcript in a cloned T-helper lymphocyte. Gene 91:185–191.

Scott BS, Becker LE, Petit TL. 1983. Neurobiology of Down's syndrome. Prog Neurobiol 21:199–237.

Schuchmann S, Müller W, Heinemann U. 1998. Altered Ca^{2+} signaling and mitochondrial deficiencies in hippocampal neurons of trisomy 16 mice: a model of Down's syndrome. J Neurosci 18:7216–7231.

Streuli C. 1999. Extracellular matrix remodelling and cellular differentiation. Curr Opin Cell Biol 11:636–640.

Sweeney JE, Höhmann CF, Oster-Granite ML, Coyle JT. 1989. Neurogenesis of the basal forebrain in euploid and trisomy 16 mice: an animal model for developmental disorders in Down's syndrome. Neuroscience 31:413–425.

Williams LR, Rylett RJ. 1990. Exogenous nerve growth factor increases the activity of high-affinity choline uptake and choline acetyltransferase in brain of Fisher 344 male rats. J Neurochem 55:1042–1049.